Quadrupolar NMR to investigate dynamics in solid materials

O'Dell, Luke A.; Ratcliffe, Christopher I.

Publisher's version / Version de l'éditeur:
https://doi.org/10.1002/9780470034590.emrstm1209
Encyclopedia of Magnetic Resonance, 2011-12-15

Quadrupolar NMR to Investigate Dynamics in Solid Materials.

emrstm1209

Luke A. O'Dell and Christopher I. Ratcliffe

Steacie Institute for Molecular Sciences, National Research Council of Canada,
100 Sussex Drive, Ottawa, Ontario K1A 0R6, Canada.

1. Introduction

Dynamics, be they vibrational, rotational or translational, are an important aspect of any solid, as they can play a major role in the overall properties of the material. NMR is perhaps the foremost technique for the study of rotational and translational motions in solid materials, and quadrupolar nuclei have a prominent role in such studies. ^{2}H NMR in particular has been, and will continue to be, a very important tool for the study of molecular dynamics, since the isotope can replace ^{1}H in countless inorganic and organic systems. ^{7}Li has also received a lot of attention, largely for studying motion in ion conducting materials. With the increased interest in the last decade in quadrupolar nuclei with larger coupling constants (brought about by access to higher magnetic fields and constantly improving experimental techniques and probe technology), there are increasing numbers of reports of dynamics observed using other quadrupolar nuclei, especially ^{17}O, but also ^{11}B, ^{14}N, ^{23}Na, ^{27}Al and ^{133}Cs, and also some transition metals involved in tetrahedral oxide ions, such as ^{185,187}Re and ^{55}Mn.

Quadrupolar NMR studies of dynamics can yield structural information such as molecular orientation with respect to a crystallographic axis, or local symmetry, and this can sometimes be used to improve or direct structural refinements. It can distinguish between static and dynamic disorder among partially occupied sites, and can indicate phase transitions and perhaps give insight into possible mechanisms for these. More directly, the NMR studies can provide rotational rate constants or correlation times, which if studied as a function of temperature yield activation energies for the motions.

The underlying behavior which makes the observation of dynamic effects possible in NMR is the modulation of the resonance frequency, brought about by any motion which causes the electric field gradient (EFG) tensor, and hence the quadrupolar interaction tensor, to undergo changes in magnitude and/or orientation [1-4]. These changes can be effected either by motion of the nucleus itself or through motion of neighboring nuclei. Since most motions are stochastic processes they are usually described in terms of an auto-correlation function $G(\tau)$:

$$G(\tau) = \overline{f(t)f(t+\tau)} \tag{1}$$

where f(t) is a function of the position and orientation of a molecule at time t and the bar represents an ensemble average. In essence, $G(\tau)$ is a measure of the fraction of molecules whose position and orientation is unchanged after a time τ. If there is motion occurring, $G(\tau)$ will decrease over time and in most cases this decay can be modeled as an exponential function with a correlation time τ_c that is inversely related to the rate of motion:

$$G(\tau) = \exp\left(-\frac{|\tau|}{\tau_c}\right) \tag{2}$$

For thermally activated processes, where the molecule must surmount an energy barrier to move between potential wells, τ_c is assumed to have an Arrhenius dependence on the activation energy (E_a) and on temperature (T):

$$\tau_c = \tau_c^0 \exp\left(\frac{E_a}{RT}\right) \tag{3}$$

from which it is seen that as T increases, τ_c decreases (and the rate of a motion increases).

As well as the rate of the motion, the geometry of the dynamic process will also determine how the motion will manifest itself in the NMR response of the quadrupolar nucleus under study, since this affects the change in orientation of the quadrupolar

interaction tensor. For example, a 180° rotation about any of the principal axes of the EFG tensor will leave it unchanged and will therefore have no effect, a situation which often arises for 2-fold molecular reorientations.

Different experimental approaches are generally used to probe motions on different timescales, e.g., two-dimensional exchange experiments for slow rates of motion, lineshape measurements for intermediate rates and relaxation measurements for fast rates. In this article, we will provide qualitative descriptions of the underlying mechanisms by which the NMR spectra of various quadrupolar nuclei can be affected by dynamics over an extremely wide range of timescales, as well as discussing the basic principles behind various experimental methods. In Sections 2-5, we focus on the quadrupolar nuclei ^{2}H, ^{14}N, ^{17}O and $^{6/7}$Li respectively, which each exhibit different NMR properties and are therefore used in distinct ways to study dynamic processes. In Section 6, we consider the effects that dynamics can have on high-resolution, multiple-quantum experiments.

2. Deuterium

2.1 T_2 anisotropy and ^{2}H spin-echo experiments

Deuterium is perhaps the most commonly exploited quadrupolar nucleus for studying molecular dynamics [5]. It is a spin I = 1 nucleus, thus the first-order quadrupolar interaction is typically the dominant perturbation and smaller interactions may often be ignored. Fortunately, the nucleus has a relatively small quadrupole moment (Q = 2.86 mbarn), and the quadrupolar splittings typically only range up to around 250 kHz. Such pattern widths can be uniformly excited and observed relatively easily on modern spectrometers, most commonly by using the quadrupolar echo pulse sequence ($\pi/2_x - \tau_d - \pi/2_y - \tau_d$ – acquire), which allows the signal acquisition to begin at the echo top and thus avoids the spectral distortions due to equipment dead-time that are associated with single-pulse experiments. Furthermore, the electric field gradient (EFG) at the deuterium site, and therefore the quadrupolar interaction tensor itself, are often axially symmetric ($\eta_Q = 0$) with the unique axis aligned along a covalent bond (e.g., a C-H bond in an organic molecule). This can greatly simplify the interpretation of results, since the interaction is then described by only two parameters (C_Q, and the angle θ

between the unique axis and B_0). Less fortunately, the ^2H isotope has a very low natural abundance (0.012 %), making isotopic enrichment necessary. This can, however, be considered an advantage in some cases, in that it allows the possibility of selective labeling, which, as well as aiding spectral resolution, can be used to probe specific sites in complex systems.

The most common method for extracting dynamic information using ^2H NMR is to record the powder pattern from a stationary sample using a spin-echo experiment, and then to compare the resultant spectral lineshape to simulations which model a Markovian jump process with a specific geometry and jump rate k [6,7]. Powder lineshapes are generally sensitive to motional rates comparable to their linewidth. At slower rates (or in the absence of motion) the lineshape is characteristic of the static quadrupolar coupling tensor **V**. In the fast motion limit (FML) the lineshape is characteristic of an effective tensor $\mathbf{V_{eff}}$, which is the population weighted average of the static tensor components in a common reference frame for all the sites visited during the motion:

$$\mathbf{V_{eff}} = \frac{\sum_{i=1\rightarrow n} \mathbf{V_i}(\alpha,\beta,\gamma)p_i}{\sum_{i=1\rightarrow n} p_i} \tag{4}$$

where p_i is the population factor of site i and the static tensor components for site i are given by:

$$\mathbf{V}(\alpha,\beta,\gamma) = R\mathbf{V_{PAS}}R^{-1} \tag{5}$$

where R is the Euler angle rotation matrix describing the coordinate transformation and $\mathbf{V_{PAS}}$ is the static tensor in its principal axis system. Thus if the static tensor is known, averaged FML lineshapes can be calculated easily for any plausible dynamic model and compared with observation. Intermediate rate dynamics, which cause lineshapes that are distorted away from typical first-order quadrupolar powder patterns, can then be calculated based on feasible model(s) and compared with experimental lineshapes to obtain rate constants or to distinguish models which give identical FML lineshapes. The geometry

used for the simulations will usually be based on knowledge of the molecular and crystal structure, e.g., a deuterium located on a methyl group might be expected to undergo C_3 rotation. If the static and FML lineshapes are both available then a dynamic model (or models, if not unique) can be developed which is compatible with the observed averaging before calculating intermediate rate lineshapes, otherwise an educated guess has to be made.

The distorted ^{2}H powder patterns that occur in the presence of intermediate motion are caused by anisotropy in the ^{2}H transverse relaxation due to the modulation of the first-order quadrupolar interaction. For such a phenomenon to occur, two conditions must be fulfilled. First, the motion must alter the orientation or magnitude of one or more principal axes of the interaction tensor, in this case the ^{2}H EFG. This alteration can be caused either by motion of the ^{2}H itself, or by motion of surrounding atoms. Secondly, the timescale for the dynamics (k^{-1}) must be comparable to the inter-pulse delay τ_d in the spin-echo pulse sequence used (or comparable to C_Q^{-1} in the limit of short τ_d values). When these conditions are fulfilled, the resonance frequencies of certain spins will change during the course of the spin-echo sequence and the corresponding signals will therefore fail to be refocused. The extent of this relaxation will be dependent on the jump rate, and also the relative orientations (with respect to B_0) or magnitudes of the EFG principal axes at each jump site. The result is that the T_2 relaxation time will differ for each crystallite orientation, and will cause the powder pattern to depart significantly from the ideal first-order quadrupolar lineshape.

In typical ^{2}H spin-echo experiments, both C_Q^{-1} and τ_d are usually on the order of 10^{-5} s, thus ^{2}H powder patterns are sensitive to motional timescales in the range 10^4 to 10^7 s^{-1}. Motions occurring on timescales much longer than τ_d will be too slow to induce anisotropic relaxation, and standard first-order lineshapes will be observed. In the fast motion regime, where the dynamics occur on timescales much shorter than τ_d, the spins will experience the FML EFG tensor, resulting in the observation of an ideal first-order pattern (or a narrow Lorentzian line for motions which average the EFG to zero). In the intermediate timescale, however, the shape of the ^{2}H powder pattern is highly sensitive to both the rate and geometry of the dynamics. For thermally-activated dynamics, jump rates can be determined from these intermediate lineshapes over a range of temperatures

(with τ_d fixed) and then used to determine the activation energy via an Arrhenius plot. Alternatively, τ_d can be varied at a constant temperature to observe the effects of the T_2 anisotropy for a fixed jump rate over a range of timescales. Such experiments can potentially provide a broad range of quantitative information on molecular dynamics (number of jump sites, respective site orientations, jump rate constants, and activation energies).

Figure 1 shows some simulated ^2H powder patterns for a methane molecule undergoing three different types of motion. For the C_2 rotation, the powder pattern shows the axially symmetric ($\eta_Q = 0$) quadrupolar pattern in the slow motion regime, which changes to a $\eta_Q = 1$ pattern in the fast limit. For the C_3 simulations, both the slow and FML lineshapes correspond to axially symmetric EFG tensors. Indeed, rotation around a single axis with C_3 symmetry or higher will always result in an axially symmetric ^2H spectrum in the FML. It should be noted here that the signal arising from the deuteron on the axis of C_3 rotation, which is neglected in the simulations, will be unaffected by this motion since this rotation does not alter the EFG tensor for this spin. For the case of tetrahedral exchange, the EFG tensor is averaged completely for jump rates of 10^5 s^{-1} and higher, leaving a narrow Lorentzian lineshape.

One significant problem that can arise in using ^2H T_2 anisotropy to probe dynamics in this way is the severe signal loss that occurs in the intermediate regime, where the transverse relaxation is extremely efficient. Figure 2 shows simulated echo intensities for the three dynamic modes in Figure 1, and the dramatic signal loss for jump rates of 10^4 to 10^6 s^{-1} (a decrease in intensity of up to an order of magnitude) is immediately apparent. As mentioned above, this intermediate region is where the lineshape shows the highest sensitivity to the dynamics. The resultant spectra can therefore exhibit rather low signal-to-noise ratios. Decreasing the echo delay τ_d can reduce this effect. Alternatively, signal enhancement techniques such as those discussed in the following sections can be used to provide a signal boost.

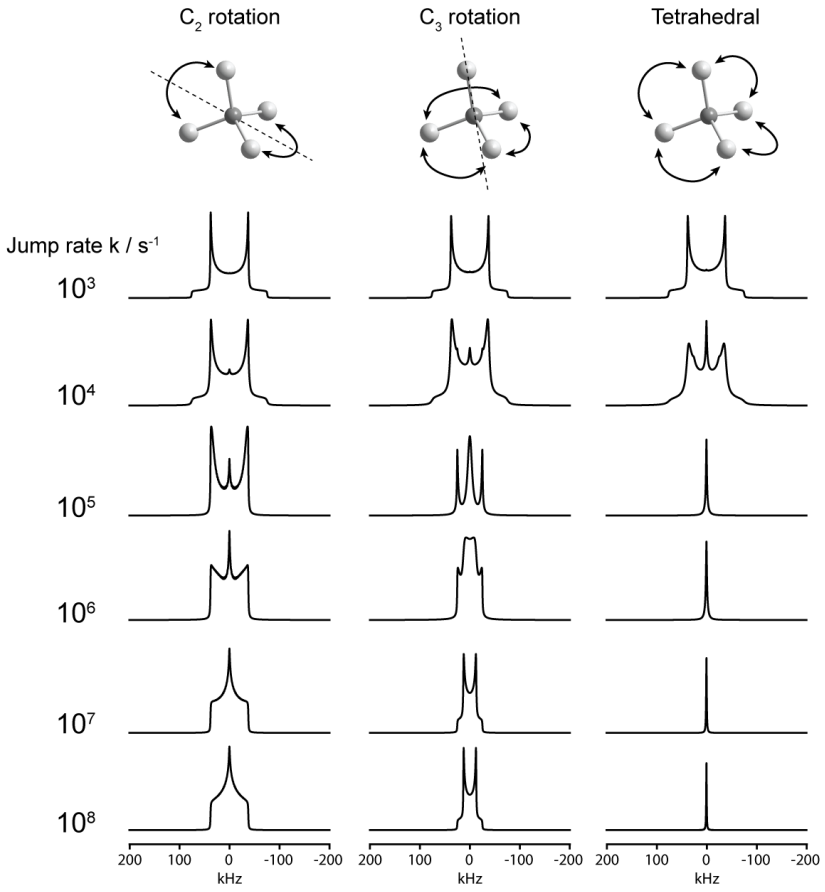

Figure 1 – Simulated ^{2}H spin-echo powder patterns arising from spins undergoing various types of Markovian jump processes as shown. Simulations were generated with the EXPRESS software [7], assuming an axially symmetric ^{2}H EFG tensor (C_Q = 100 kHz) and a quadrupolar-echo pulse sequence with a 50 µs inter-pulse delay. For the C_3 rotation, the signal from the axial deuterium site is neglected. Spectral intensities are not to scale.

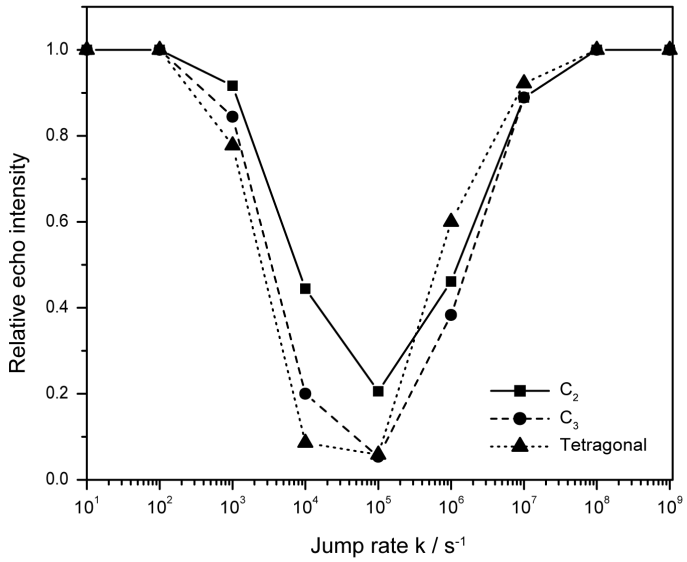

Figure 2 – Normalized spin-echo intensities vs. jump rates for the simulations shown in Figure 1.

2.2 Magic angle spinning

In magic angle spinning (MAS) ^{2}H NMR experiments, the first-order quadrupolar broadening is averaged, leaving a manifold of spinning sidebands for each unique deuterium site that can often be resolved on the basis of differences in the second-order quadrupolar and isotropic chemical shifts. Such a method can therefore increase both the sensitivity and resolution of ^{2}H spectra. In studying dynamics, MAS also has the advantage of extending the range of motional timescales that can be probed [8]. In Figure 3, the manifold of spinning sidebands in simulated MAS spectra of a system undergoing C_3 rotation (as in Figure 1) is seen to be sensitive to a similar range of jump rates as the static powder pattern. On closer inspection, however, the widths of the sidebands themselves are seen to be sensitive to a greater range of jump rates. For example, the width of the most intense spinning sideband is noticeably different for jump rates of 10^2 and 10^3 s^{-1}, while these jump rates are indistinguishable on the basis of the static spin-echo powder patterns. This additional sensitivity of MAS spectra to motional processes arises because the dynamics interfere with the refocusing of the anisotropic interactions by the sample rotation [9]. The disadvantage of this phenomenon is that excessive broadening of the spinning sidebands in the intermediate regime can cause loss

of resolution for sites with different isotropic shifts. Spinning sidebands may also provide more precise measurements of dynamics when the sample is spun at a small offset from the magic angle. In this case, a scaled quadrupolar interaction is re-introduced, giving each spinning sideband a characteristic shape that is dependent on the dynamics (particularly those occurring in the kHz regime) and may be simulated to extract this information [10].

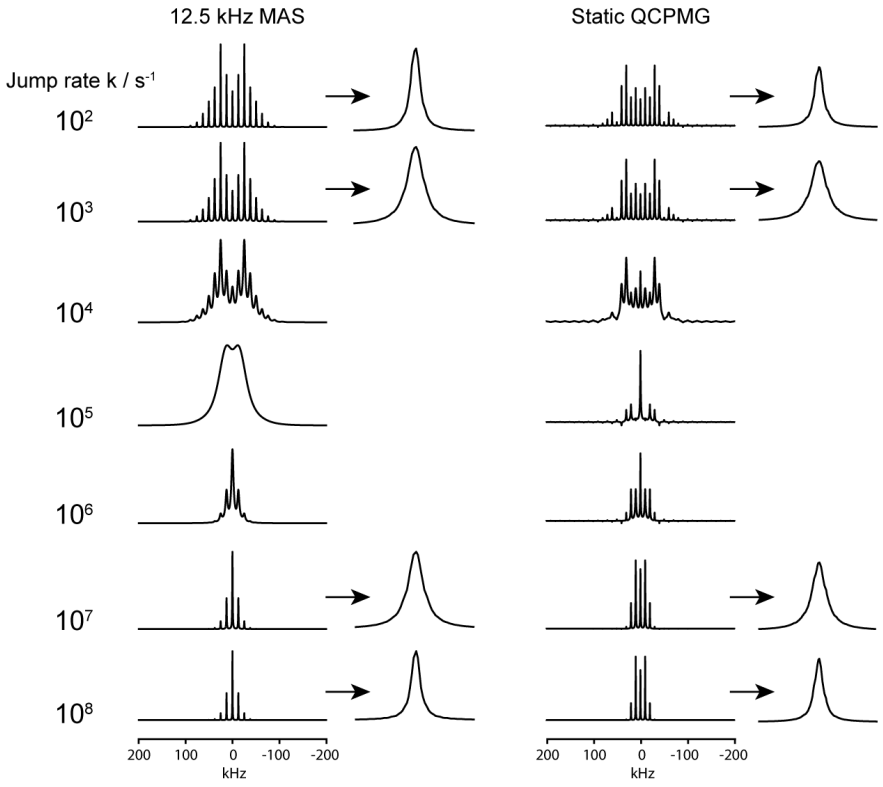

Figure 3 – Simulated ^{2}H MAS (left) and static QCPMG (right) spectra for the system undergoing C_3 rotations shown in Figure 1 (the axial ^{2}H is again neglected). The MAS simulations used a rotor frequency of 12.5 kHz, and the QCPMG simulations have a spikelet separation of 10 kHz. For certain jump rates, horizontal expansions of the most intense sidebands/spikelets are also shown as indicated by the arrows. Simulations were generated using EXPRESS [7].

2.3 QCPMG

QCPMG is now a very commonly used signal enhancement pulse sequence in solid-state NMR. Several variations of this pulse sequence exist, the defining feature being a repeating loop containing a refocusing pulse and an acquisition period, allowing the spin-echo to be re-recorded over the full timescale of the transverse relaxation/dephasing. A Fourier transform of the echo train results in a spectrum consisting of narrow "spikelets" whose manifold reproduces the approximate shape of the powder pattern. The QCPMG experiment therefore samples a broader range of timescales than a single spin-echo, and so can extend the range of motional timescales that can be studied using ^{2}H based on differences in the linewidths of the spikelets (see Figure 3) [11]. While both MAS and QCPMG offer significant increases in sensitivity, the most significant difference between the techniques is that QCPMG only ever results in a single spikelet manifold for all signals, thus does not offer the shift-based resolution advantage of MAS.

A recent study of methyl group rotation in the hydrophobic core of a protein provides an illustration of the advantages of QCPMG signal enhancement [12]. ^{2}H spectra were recorded from a powder sample of protein at various cryogenic temperatures, with a single methyl group of a hydrophobic core residue selectively labeled with ^{2}H (Figure 4). All three motional regimes were observed. In the FML (119 K), the methyl group rotation results in a relatively narrow spikelet manifold corresponding to a motionally-averaged EFG tensor. At 84 K, the spikelet manifold narrowed significantly and the amount of signal dropped, indicating motion on the intermediate timescale. At 31 K, a spikelet manifold corresponding to a relatively broad axial pattern was observed, indicating the freezing-out of the methyl rotation.

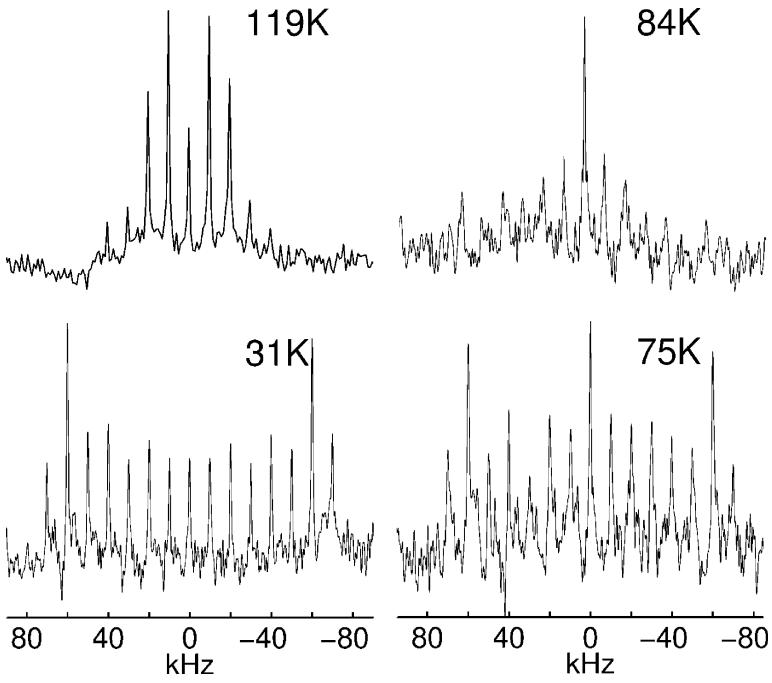

Figure 4 – ^{2}H QCPMG spectra obtained at 11.7 T and at temperatures shown from a powder sample of chicken villin headpiece subdomain (HP36), selectively ^{2}H-labeled at a single methyl group of residue L69. 1024, 3040, 512, and 128 scans were acquired for the spectra at 119, 84, 75 and 31 K respectively. Reproduced with permission from reference 12. Copyright 2010 American Chemical Society.

2.4 T_1 anisotropy and inversion recovery experiments

Dynamic modes such as those discussed in the previous sections are also capable of causing anisotropies in the (Zeeman) spin-lattice relaxation time T_{1Z} [13]. Whereas transverse relaxation is induced by dynamics whose characteristic frequencies are on the order of the anisotropic interactions present (i.e., the C_Q in the case of ^{2}H, which is on the order of 100 kHz), spin-lattice relaxation is caused by interactions fluctuating at or close to the Larmor frequency (~ 61 MHz for ^{2}H at a field of 9.4 T). Specifically, T_{1Z} depends on the two spectral densities $J_1(\omega_0)$ and $J_2(2\omega_0)$ (which are themselves dependent on the motional correlation time and are orientation dependent under anisotropic motion), and ^{2}H T_{1Z} measurements can therefore provide access to very fast motional rates (up to ~ 10^{11} s^{-1}):

$$\frac{1}{T_{1Z}} = \frac{3\pi^2}{2} C_Q^2 (J_1(\omega_0) + 4J_2(2\omega_0)) \tag{6}$$

The simplest way of observing T_{1Z} anisotropy experimentally is using an inversion recovery pulse sequence of the form $\pi - t_1 - \pi/2 -$ acquire, where the magnetization is stored anti-parallel to B_0 for a variable recovery time t_1, and subsequently observed using a $\pi/2$ pulse (or, more typically for ^{2}H, a spin-echo sequence). Figure 5 shows a simulated T_{1Z} anisotropy profile for the ^{2}H C_3 rotation discussed above, at 9.4 T and with a jump rate of 10^9 s^{-1}. Such a jump rate is too fast to affect the spin-echo lineshape in a standard experiment, resulting in an axially symmetric FML powder pattern. In an inversion recovery experiment, however, the T_{1Z} anisotropy can be measured by recording spectra over a range of t_1 values, and the shape of the T_{1Z} anisotropy will be dependent on both the rate and geometry of the dynamics. We note that these simulations include only the effects of the C_3 dynamics, and neglect other possible causes of relaxation such as lattice vibrations, although in most cases the relaxation mechanism in ^{2}H will be dominated by the quadrupolar interaction. T_1 behavior can also distinguish between dynamic models which give the same FML lineshape, e.g., Markovian jumps or smooth rotational diffusion about the C_3 axis.

It should also be noted that the anisotropy in the relaxation of quadrupolar order, in which a single transition is inverted, is also sensitive to dynamics. This state can be created using a Jeener-Broekaert pulse sequence [14]. For fast motions, this relaxation can provide complementary information to T_{1Z} measurements since its associated relaxation time T_{1Q} is dependent on only one spectral density $J_1(\omega_0)$ [7]:

$$\frac{1}{T_{1Q}} = \frac{9\pi^2}{2} C_Q^2 (J_1(\omega_0)) \tag{7}$$

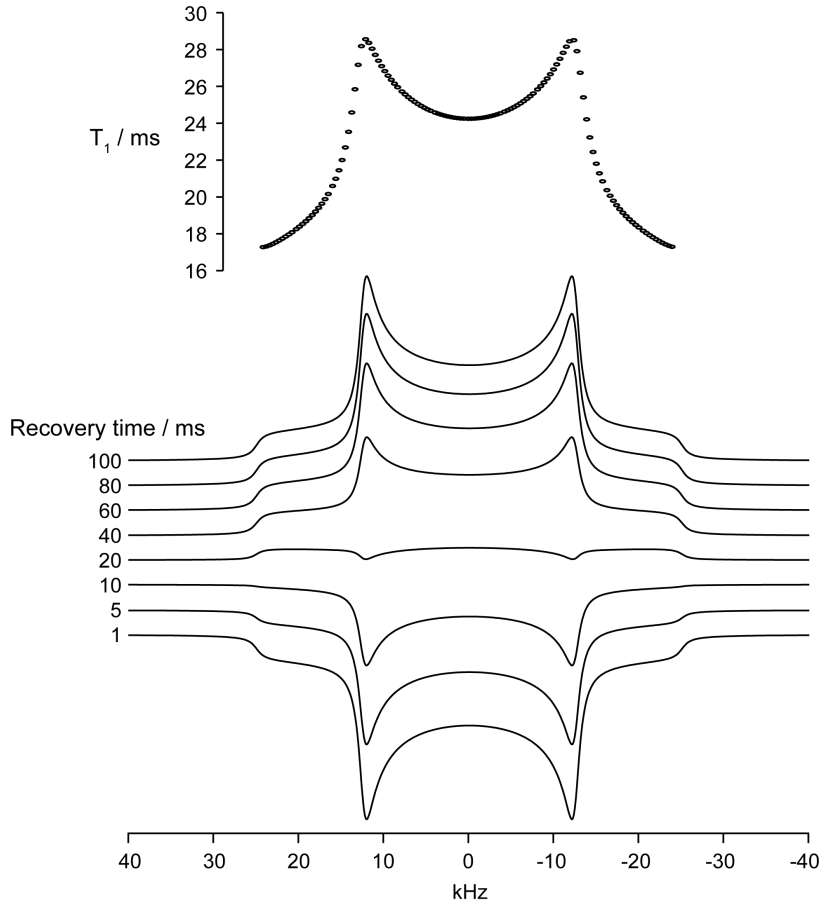

Figure 5 – Top: simulated T_1 anisotropy for a ^2H system (C_Q = 100 kHz, η_Q = 0, B_0 = 9.4 T) undergoing C_3 rotation (as in Figure 1) with a jump rate of 10^9 s^{-1} (axial deuteron is again neglected). Bottom: corresponding inversion recovery spectra with various recovery times. Simulations were generated using EXPRESS [7].

This allows both spectral densities to be quantified [15], and also makes T_{1Q} relaxation a useful probe for quantifying very slow reorientations ($\sim$ 1 s^{-1}), since it is less sensitive to rapid vibrational motions than T_{1Z} [16]. Note also that the QCPMG retains longitudinal relaxation anisotropy while MAS does not [17], thus QCPMG can be useful in improving the sensitivity in such experiments.

2.5 Two-dimensional exchange experiments

The fitting of simulated spin-echo lineshapes or relaxation anisotropies to experimental ^{2}H data usually necessitates some prior knowledge of the molecular structure in order to guess potential dynamic models. Two-dimensional exchange experiments provide an alternative approach where motional rates and geometries can be inferred solely from the experimental data [18]. An example spectrum is shown in Figure 6, obtained from dimethylsulfone. In this molecule, the methyl groups undergo rapid rotation such that the ^{2}H powder pattern corresponds to an axially symmetric EFG tensor aligned along the S-C bond. The molecule also undergoes a slower two-site jump process about its C_2 symmetry axis that alters the orientation of this ^{2}H EFG by 106°. In the exchange spectrum, the main peaks along the diagonal map out the static, axially-symmetric quadrupolar pattern, while the two-site jump process that occurs during the mixing period gives rise to off-diagonal ridges. Crucially, these ridges show characteristic shapes that depend explicitly on the motional geometry, allowing the flip angles and number of jump sites to be deduced directly from the spectrum [18].

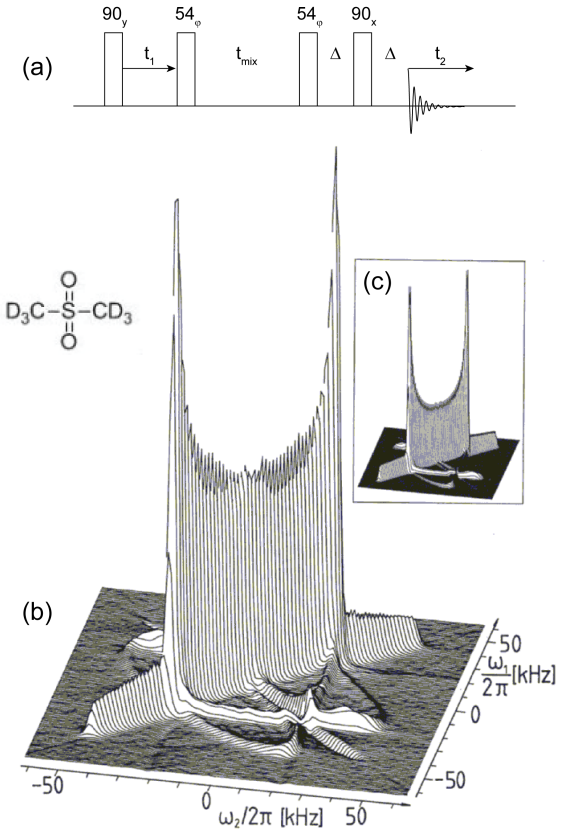

Figure 6 – (a) Pulse sequence used to acquire the ^{2}H two-dimensional exchange spectrum (b) from dimethylsulfone (molecule shown inset). (c) Simulated spectrum taking into account the two-site 106° flipping mechanism. Reproduced with permission from reference 18. Copyright 1986 Elsevier.

3. Nitrogen-14

3.1 T_2 anisotropy and ultra-wideline powder patterns

The ^{14}N isotope is also a spin I = 1 nucleus, and so the above techniques are in principle also applicable to this nucleus. Unfortunately, this nucleus has a quadrupole moment that is seven times larger than ^{2}H (20.44 mbarn), thus the broadening due to the first-order quadrupolar interaction is usually extremely large (several MHz) and such broad spectra can be very difficult to observe [19]. Dynamics studies employing this nucleus are therefore rather scarce. Spin-echo experiments using standard excitation pulses have been carried out on systems where the nitrogen sites have a local symmetry that is close to tetrahedral, giving rise to small C_Q values, such as in choline salts [20]. Motionally-averaged ^{14}N quadrupolar splittings have also been observed in partially-oriented systems such as liquid crystals or lipid bilayers. Such splittings are often directly proportional to the ordering parameter describing the rotational dynamics present in these systems, but again, such cases generally involve nitrogen sites with symmetric environments and small C_Q values. The majority of nitrogen sites feature C_Q values in excess of 1 MHz, and these require more advanced experimental methods [19].

The jump rate for the molecular flipping mechanism in crystalline urea (C_Q = 3.86 MHz and η_Q = 0.28) has recently been determined using ultra-wideline ^{14}N NMR as $k = 7 \times 10^3$ s^{-1} at room temperature [21]. Frequency-swept pulses combined with QCPMG were used to excite a broad region of the powder pattern where the T_2 anisotropy was most pronounced (Figure 7). This outermost region of the powder pattern corresponds to crystallite orientations in which the EFG principal axis V_{33} is parallel to B_0, thus the molecular flipping in these crystallites does not alter the EFG orientation and the motion does not induce transverse relaxation for these spins. The outermost edges of the pattern are therefore selectively enhanced by the QCPMG protocol, as seen in the simulations in Figure 7. Fitting of these simulated lineshapes to the experimental spectra provided jump

rate constants in good agreement with those measured using other techniques, demonstrating that the simple approach described in Section 2.1 holds, at least to a good approximation, even for very large quadrupolar interactions.

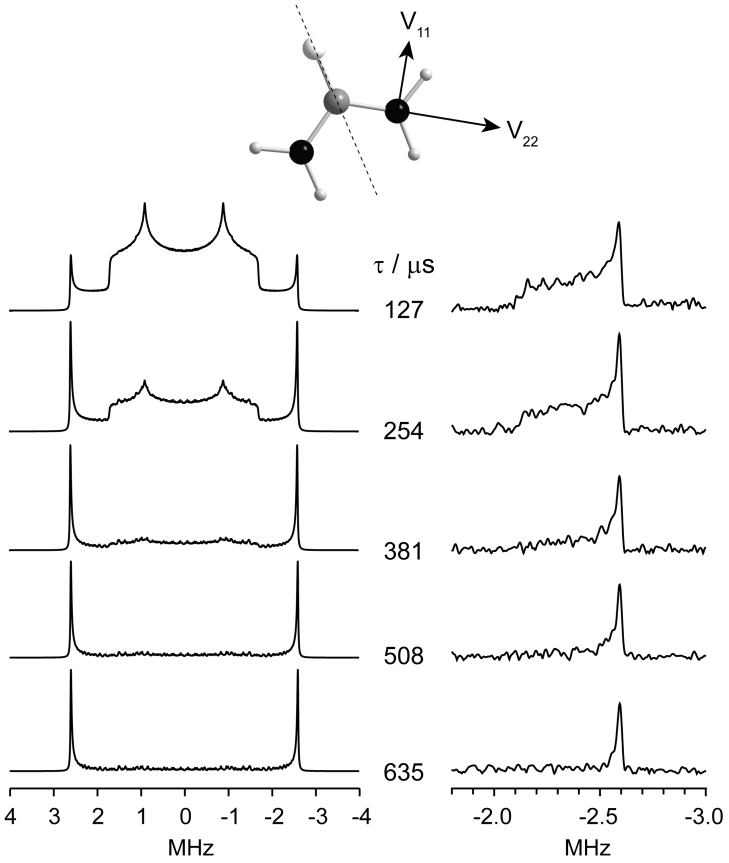

Figure 7 – Simulated (left) and experimental (right) ^{14}N spectra obtained from urea at 21.1 T and at room temperature. The molecule is shown inset, along with the orientation of two of the ^{14}N EFG principal axes (the third, V_{33}, is perpendicular to the molecular plane). Simulations were made using EXPRESS [7] with a jump rate of 7×10^3 s^{-1} and inter-pulse delays as shown. Experimental spectra (recorded at the low-frequency edge of the ultra-wideline powder pattern) were made by extracting single echoes from a QCPMG train at corresponding τ values and Fourier transforming these individually. Reproduced from reference 21 by permission of the Royal Society of Chemistry.

3.2 Hole-burning methods

Saturation or inversion recovery methods are usually used to study very fast dynamics via their effect on the spin-lattice relaxation rate. However, they may also be used to probe very slow motions occurring at timescales on the order of the T_1 relaxation time itself. The hexamethylenetetramine (HMT) molecule (^{14}N C_Q = 4.41 MHz, η_Q = 0) in its crystalline form undergoes tetrahedral jumps at a rate of ~10 s^{-1} at room temperature, moving the ^{14}N EFG tensor between four orientations. Such motion is far too slow to be observed as a change in the shape of the ^{14}N powder pattern, but its effects have been observed using saturation-recovery experiments applied to a narrow region of the ultra-wideline powder pattern (referred to as hole-burning) [22]. Specifically, a train of transition-selective pulses can be used to saturate a 4 kHz wide region of the powder pattern which can then be monitored over time using a conventional spin-echo pulse sequence. After a single train of pulses, a set of ^{14}N spins corresponding to a specific set of EFG orientations is saturated. The EFG orientations of these saturated spins are then altered by the molecular reorientation, which also brings unsaturated magnetization (i.e., ^{14}N spins previously at other EFG orientations) into the hole region. For the four-site jump process in HMT, three quarters of the magnetization is therefore quickly recovered due to the dynamics alone, followed by a much slower recovery of the remaining

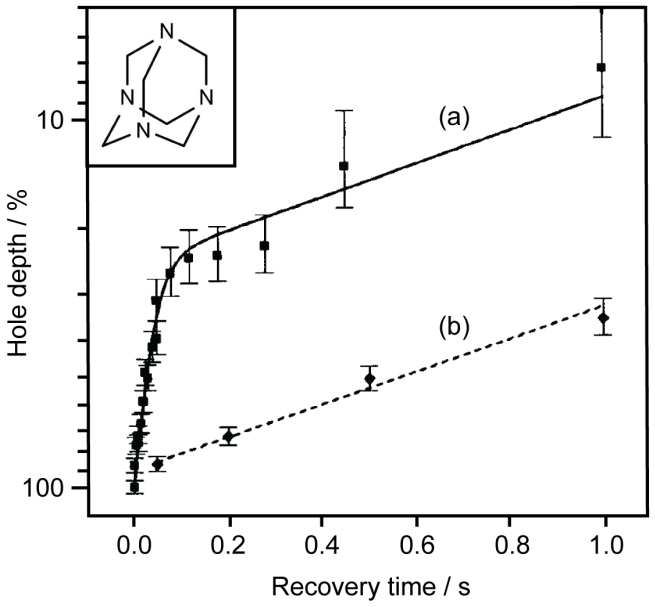

Figure 8 - Recovery of a narrow region of saturated ^{14}N magnetization in hexamethylenetetramine (molecule shown inset) at 7.05 T as a function of time after (a) a single train of saturation pulses and (b) 16 saturation trains. Solid and dotted lines show fits derived from numerical expressions. Reproduced with permission from reference 22. Copyright 1997, American Institute of Physics.

magnetization by ordinary spin-lattice relaxation (Figure 8a). Note that the fraction of magnetization recovered in the initial stage provides an immediate quantification of the number of jump sites. Alternatively, all four sets of EFG orientations can be saturated, after which the recovery of magnetization occurs by spin-lattice relaxation only (Figure 8b).

3.3 T_1 measurements

T_1 relaxation times can be measured relatively easily from nitrogen sites with high symmetry or fast dynamics where the ^{14}N quadrupolar interaction is absent or extremely small. For example, in ionic solids such as NaCN, the CN^- ions can undergo rapid rotation and therefore exhibit very narrow linewidths despite the relatively high C_Q value of the stationary ion (~4 MHz). The rapid EFG fluctuations caused by this rotation lead to very efficient relaxation, and the departure from cubic symmetry caused by orientational disorder or defects present in the lattice can leave very small residual quadrupolar broadening which can be observed using the quadrupolar echo sequence. The spin-lattice relaxation cannot therefore be directly inferred from the natural linewidths ($1/T_2$*), but correlation times for the rotation can still be easily ascertained from inversion recovery T_1 measurements, allowing the very fast ion rotation rate ($\tau \approx 10^{-10}$ s) to be measured [23].

4. Oxygen-17

4.1 Central transition lineshapes

Since the majority of quadrupolar nuclei have a half-integer spin number with a corresponding central transition (CT) that is free of first-order quadrupolar broadening, it is of interest to extend the ^2H spin-echo methods outlined above to such systems in order

to access dynamics in systems which may not contain hydrogen. In this section we will consider ^{17}O (I = 5/2) as an exemplary half-integer quadrupolar nucleus. Oxygen is clearly an element of considerable importance, so it is rather unfortunate that ^{17}O has a very low natural abundance (0.038 %) and a relatively low gyromagnetic ratio (ν_0 = 54.2 MHz at 9.4 T). Isotopic enrichment is therefore usually required for studies of this nucleus. On the plus side, the nucleus has only a moderate quadrupole moment (−25.6 mbarn) and a reasonably large chemical shift range (~1000 ppm), meaning that solid-state spectra can often be obtained (under MAS) with a relatively high resolution, particularly at high magnetic field strengths.

^{17}O CT NMR spectra obtained from powder materials under either static or MAS conditions show anisotropic broadening due to the second-order quadrupolar interaction (as well as chemical shift anisotropy in the case of static powders). These anisotropic interactions, like the first-order quadrupolar interaction for ^{2}H, can be modulated by dynamic processes giving rise to anisotropic relaxation, altering the shape of the powder pattern and thus constituting a mechanism by which motional rate constants and geometries can be measured. Figure 9 shows simulated CT lineshapes for ^{17}O spins in an MO_4 unit undergoing various dynamic mechanisms. As with the ^{2}H experiments discussed above, the ^{17}O CT lineshapes are sensitive to motions at intermediate rates (~ 10^3 to 10^7 s^{-1}) which are comparable to the size of the second-order quadrupolar interaction (C_Q^2/ν_0). The satellite transitions (STs) are sensitive to motions at much faster rates (on the order of C_Q). Note that the centerband and spinning sidebands in the MAS simulations consist of powder patterns due to incomplete averaging of the second-order quadrupolar interaction, and that these powder patterns are also sensitive to the dynamics.

Motions in the slow-regime do not affect the CT spectra, leaving standard second-order powder patterns. Interestingly, motions in the fast regime produce powder patterns that, while narrowed, do not correspond to typical second-order quadrupolar lineshapes and cannot be simulated using standard CT powder patterns [24]. This is because the second-order quadrupolar interaction features both second- and fourth-rank terms, which are weighted differently when averaged by fast motion [25]. Such fast-regime lineshapes can therefore only be reproduced using simulations which take the dynamics into account. A related observation, apparent by comparing Figures 9 and 1, is that fast

tetrahedral exchange does not completely average away the second-order quadrupolar interaction as it does for the first-order interaction. This is due to the fourth-rank anisotropy terms, which have lower symmetry. For motional rates on the order of C_Q^2/ν_0, dynamics with icosahedral or higher symmetry are required for the anisotropic terms to become fully averaged, while the isotropic second-order quadrupolar shift, which has no angular dependence, will remain [25]. However, for much faster rates (on the order of ν_0 or greater) both the anisotropic lineshape and the second order shift are averaged, so that eventually even averaging over tetrahedral sites will give a narrow lineshape at the true isotropic chemical shift [26]. It should be noted that the chemical shielding anisotropy is neglected from the simulations in Figure 9, which at high magnetic fields can be similar in size to the second-order quadrupolar broadening and can therefore also play a significant role in determining the shape of the motionally-averaged lineshape (except under MAS where this interaction is averaged out) [24]. As with ^{2}H NMR, the use of inversion-recovery [27] or QCPMG methods [28] can increase the range of motional timescales accessible by central transition spectra.

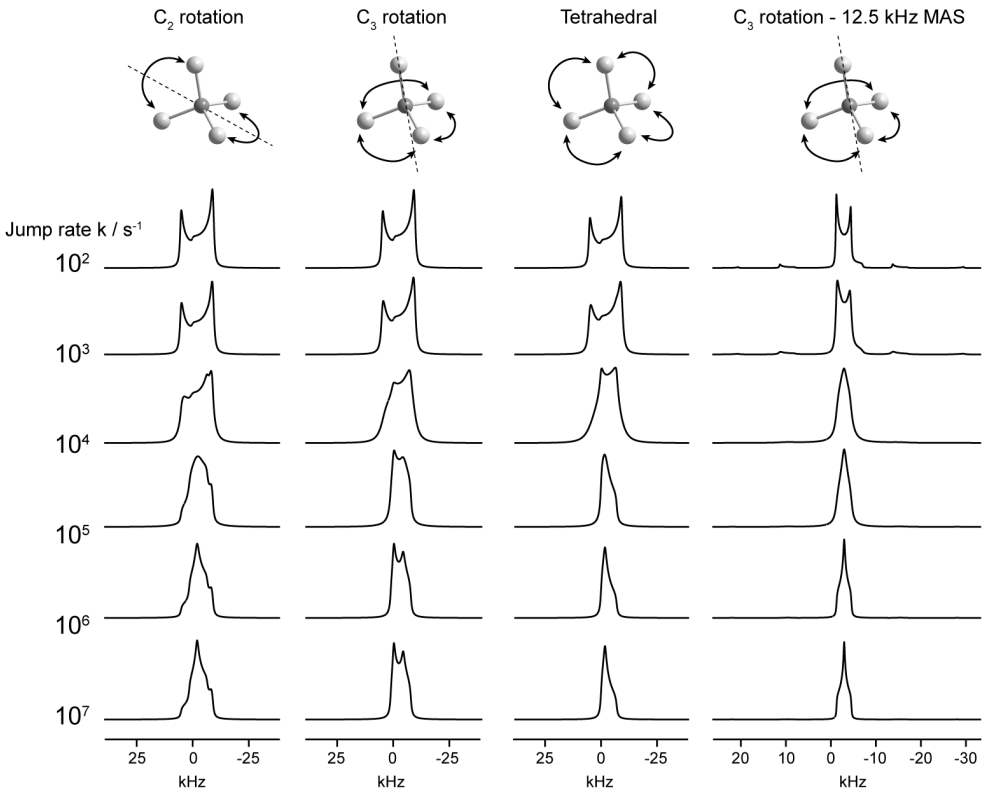

Figure 9 – Simulated ^{17}O central transition NMR spectra for various dynamic modes of an MO_4 unit shown at the top. Simulations were generated using EXPRESS [7] for a ^{17}O spin at 9.4 T with C_Q = 5 MHz and η_Q = 0. No chemical shielding anisotropy was included. As before, the signal from the axial site in the C_3 rotation model is neglected.

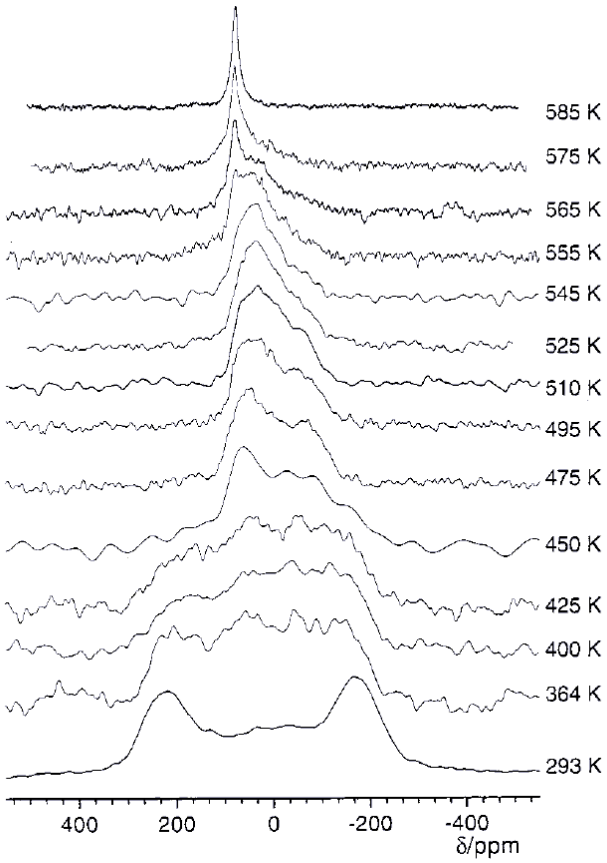

Figure 10 – Variable temperature ^{17}O NMR obtained from a static powder sample of Na_3PO_4 at 7 T. Reproduced with permission from reference 29. Copyright 2001 American Chemical Society.

^{17}O NMR has been used in this way to characterize the rotation of PO_4^{3-} anions in the low temperature phase of Na_3PO_4 [29]. In this system the ^{17}O EFG tensor was found to be axially symmetric and oriented along the P-O bond. The static ^{17}O NMR spectrum

was observed to undergo dramatic changes in shape upon heating (Figure 10), leading ultimately to a motionally-narrowed Lorentzian lineshape at 585 K which was best acquired using non-selective excitation pulses. The anisotropic lineshapes over the temperature range 425 to 525 K were shown to fit most accurately to simulations in which the anions undergo preferred C_3 rotation around one P-O bond with much slower C_3 rotation around the remaining 3. This allowed the activation energy for this preferred rotation to be obtained, and the phosphate ion motion was then correlated with that of the Na^+ cations (which undergo translational diffusion, studied via two-dimensional nutation spectra) [29].

In another example, the dynamics of water molecules in ice and THF clathrate hydrate have been followed using ^{17}O NMR lineshapes [30]. In this system, each O atom has a roughly tetrahedral arrangement of four hydrogen bonds, in which it is bonded directly to two H atoms and accepts H-bonds from two other water molecules. Interestingly, in this particular case the O atom itself does not move, but the surrounding EFG changes among six octahedral orientations due to movement of the H atoms. This may be contrasted with ^2H which does move and the orientation of its EFG tensor changes among four tetrahedral orientations. For ice, ^2H NMR lineshapes as a function of temperature show complete narrowing of the first-order lineshape to a pseudo-isotropic lineshape, corresponding to an effective C_Q of zero [31]. ^{17}O NMR, however, shows narrowing of the CT to a new *anisotropic* lineshape which is still present at the melting point, i.e., there is incomplete averaging of the second-order lineshape (Figure 11a). In THF clathrate hydrate the water dynamics are significantly faster, so that lineshapes similar to those seen in ice occur at a temperature about 40-50 K, and in this case further CT lineshape changes can be followed before melting occurs (Figure 11b). It is clear that although the lineshape initially averages towards the expected anisotropic lineshape, it then gradually becomes isotropic in shape, but this "isotropic" line retains a second-order shift as illustrated by the spectrum of the hydrate at 270 K where liquid THF solution and solid THF hydrate coexist (Figure 11c). The liquid line is considerably sharper and very close to the shift of water, whereas the broader "isotropic" line of the hydrate is centred at -194 ± 3 ppm, very close to the second-order shift of -193.6 ppm determined from the low temperature static lineshape. It would seem that the change to

an “isotropic” lineshape is associated with the onset of averaging of the first-order interaction (ν_Q is only 964.5 kHz, where $\nu_Q = 3C_Q/2I(2I-1)$ and $2\nu_Q$ gives the total width of the powder lineshape for the $\pm1/2 \leftrightarrow \pm3/2$ satellite transitions), and retention of the full second-order shift indicates that the rate is still significantly slower than the resonance frequency (ν_0 = 40.68 MHz). This same motion also has an effect on the ^{131}Xe NMR lineshapes of xenon as a guest in clathrate hydrates [32], where the Xe is an example of a spectator nucleus subjected to changes in EFG due to motions of surrounding molecules. We note that dynamics have also been observed to cause the second-order shift to decrease to zero for ^{23}Na in Na_3PO_4/Na_2SO_4 solid solutions at high temperatures [33]. These examples demonstrate that care must be exercised in judging whether one has the true isotropic chemical shift for apparently isotropic CT lines of non-integer quadrupolar nuclei, and spectra obtained at multiple fields can be used to distinguish second-order shifts from true isotropic shifts.

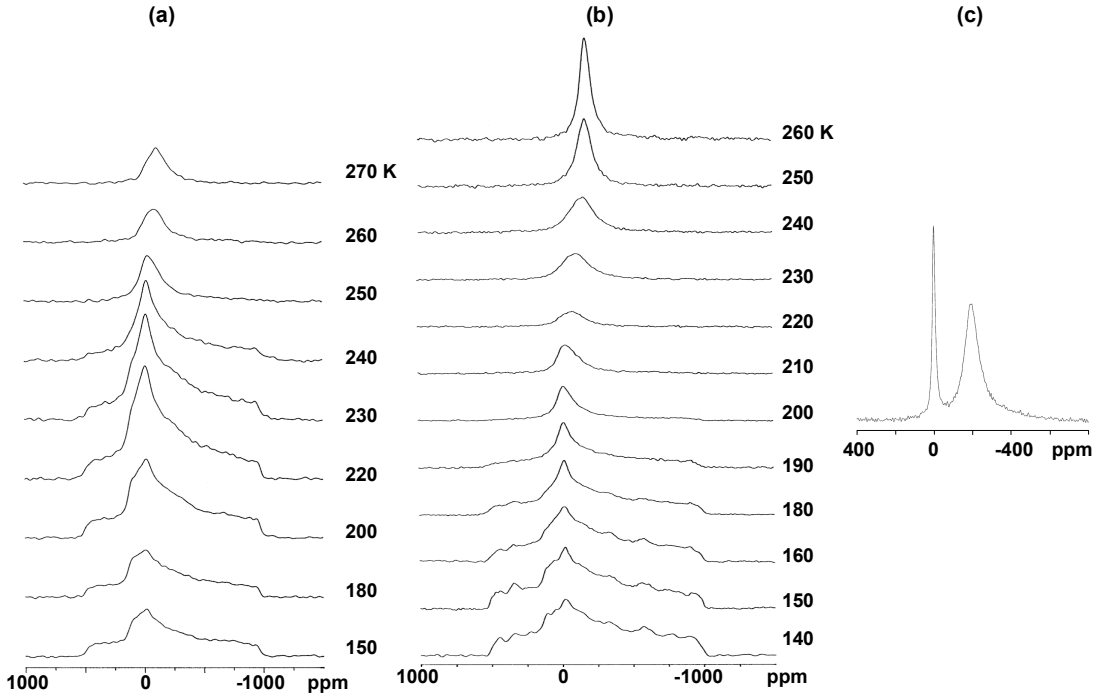

Figure 11 –Static ^{1}H-decoupled ^{17}O NMR CT transition spectra as a function of temperature at 7 T of (a) ice, (b) THF clathrate hydrate, (c) A spectrum obtained at about 270 K after partial melting of the THF hydrate. The liquid shows an isotropic chemical shift whereas the apparently "isotropic" hydrate line still also has a second-order quadrupolar shift [30].

4.2 Exchange experiments and spin-lattice relaxation

In systems where second-order quadrupolar broadening is minimal and individual oxygen sites are well resolved by MAS, exchange occurring on a similar timescale to the difference in resonance frequencies can be observed directly in one-dimensional spectra as a broadening (intermediate regime) or coalescence (fast regime) of the two peaks to an averaged position in the spectrum. Such a process has been used to observe the hopping of oxide ions between sites in α-$Bi_4V_2O_{11}$ at rates on the order of 10^4 s^{-1} [34]. In the same study, it was also noted that spinning sidebands arising from ^{17}O satellite transitions were also sensitive to dynamics, broadening and disappearing upon heating as motions on the order of the C_Q or MAS frequency prevent their formation [34], a process analogous to the ^{2}H experiments discussed in Section 2.2.

Slower exchange can be observed using two-dimensional exchange spectroscopy. An example of this is shown in Figure 12, where exchange between all four oxygen sites in an isotopically-enriched sample of ZrW_2O_8 is evidenced by the appearance of off-diagonal cross-peaks [35]. The mixing time used in this experiment was 50 ms, indicating that the WO_4 groups rotate on a timescale of ~ 10 s^{-1}. Hopping rate constants can in principle be extracted via the relative intensities of the cross-peaks, but the quantification of jump rates and activation energies from such magnetization transfer experiments is complicated since both the dynamic exchange process and spin-lattice relaxation effects must be considered. The latter process is multi-exponential for half-integer quadrupolar nuclei due to the large number of spin states between which coherences can be exchanged, and analysis is further complicated by the presence of two distinct mechanisms driving the relaxation (modulations of the quadrupolar interaction as well as the local magnetic field) [36].

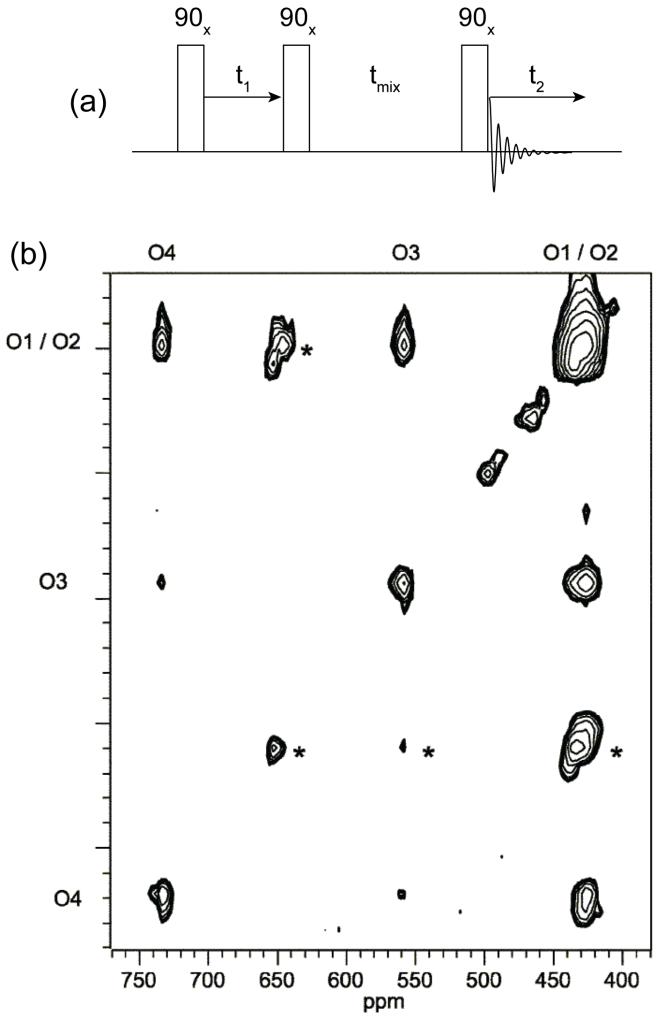

Figure 12 – (a) The basic two-dimensional exchange (EXSY) pulse sequence, where t_1-encoded chemical exchange occurs between longitudinal components of magnetization during t_{mix}. (b) A ^{17}O EXSY spectrum obtained at 11.7 T from a sample of ^{17}O-enriched ZrW_2O_8 at 57 °C and spinning at 14.5 kHz MAS. Off-diagonal peaks indicate exchange between sites O3, O4 and O1/O2, the latter sites being unresolved. Asterisks indicate spinning sidebands. Reproduced from reference 35 by permission of the Royal Society of Chemistry.

For a spin I nucleus, the spin-lattice relaxation can be described by up to 2I distinct relaxation times arising from the 2I rate equations that define the transition

probabilities between the various energy levels [37]. For I > ½ nuclei experiencing a non-zero quadrupolar interaction, and assuming that the first-order quadrupolar interaction is the dominant relaxation mechanism, all Δm = 2 transitions and Δm = 1 satellite transitions will each contribute with transition probabilities aW_2 and bW_1 respectively, where *a* and *b* are factors specific to the two levels involved in the transition as well as the direction of the transition [37,38]. When the magnetic relaxation mechanism is dominant, relaxation is mediated only by Δm = 1 transitions, and the central and satellite transitions will each contribute transition probabilities dependent on a single rate process W. In both cases, the relaxation is typically multi-exponential. Usually these complex, general solutions can be simplified, for example in the case of a spin I = 5/2 nucleus undergoing quadrupolar relaxation the description of the spin-lattice relaxation can be reduced to just three relaxation times by assuming that the Boltzmann population differences between all adjacent levels are equal and also noting symmetries in the rate equations, e.g., the +5/2 ↔ +3/2 and −5/2 ↔ −3/2 transitions [37]. Note that W_1 and W_2 are functions of the EFG orientation as well as temperature, which further complicates the description of quadrupolar relaxation in powder samples.

5. Lithium

With the exception of Francium, all of the alkali metals have quadrupolar nuclei that can be studied relatively easily using solid-state NMR. The most commonly utilized alkali metal in NMR studies of dynamics is lithium, and this is due both to its favorable NMR properties and the importance of the Li^+ ion in conducting materials. A 2007 review provides a very extensive overview of the various ways in which lithium NMR has been used to provide important information in such systems [39].

^{7}Li has a spin I = 3/2, a high natural abundance (92.4 %) and a moderately sized quadrupole moment (−40.1 mbarn). The second isotope, ^{6}Li, has a spin I = 1, but because of its very small quadrupole moment (−0.81 mbarn), this nucleus is also amenable to study by NMR. Studying dynamics using both nuclei can be advantageous as it allows dynamic models to be checked against the different properties of each spin. Since isotope effects on the mobility of lithium ions are expected to be negligible, the same dynamic model should apply to both lithium isotopes. For example, lithium ion

conduction in Li_3N has been studied using the second-order quadrupolar shift of ^7Li and the relaxation rates of both ^7Li and ^6Li, with each set of results independently confirming a proposed conduction model [40].

The second-order quadrupolar shift for ^6Li is negligible due to its very small quadrupole moment, thus this isotope is best for determining isotropic chemical shifts. Despite a small inherent chemical shift range (~ 10 ppm for diamagnetic materials), the second-order quadrupolar interaction is small for both isotopes, so MAS spectra with good resolution can often be obtained from both nuclei, and more advanced MAS methods can then be applied (e.g., ^6Li exchange experiments have been used to characterize Li^+ hopping rates in Li_4SiO_4 [41]). The resolution can be vastly improved in paramagnetic materials due to large hyperfine shifts induced by the Fermi contact interaction. Quadrupolar splittings are usually not resolved in ^6Li spectra, but they may be resolved via the satellite transition spinning sidebands in ^7Li MAS spectra. However, many lithium ion conductors exhibit disorder on the lithium sub-lattice so that even in the absence of motion the quadrupolar splittings will be smeared out by distributions in the quadrupolar parameters.

For natural abundance systems, MAS linewidths for ^7Li may be broader than for ^6Li due to homogeneous broadening caused by the homonuclear dipolar interaction, a phenomenon that may be reduced by ^6Li enrichment. The linewidths can also be affected by motional narrowing as the sample temperature is increased. This is caused by the averaging of the dipolar and quadrupolar interactions as the ions become increasingly mobile, and the correlation time for the translational motion can be extracted from the linewidths $\Delta\nu$ using the expression [39,42]:

$$\tau_c(T) = \frac{1}{2\pi\alpha.\Delta\nu(T)} \tan\left[\frac{\pi}{2}\left(\frac{\Delta\nu(T)}{\Delta\nu_{RL}}\right)^2\right] \tag{8}$$

where $\Delta\nu_{RL}$ is the rigid lattice linewidth (i.e., in the absence of motion) and α is a factor approximately equal to 1.

In general, T_1 relaxation measurements can be used to probe dynamics occurring on the timescale of the Larmor frequency (10^6 to 10^8 s^{-1}), while $T_{1\rho}$, i.e., the relaxation

under a spin-lock field in the rotating frame, can be used to probe slower motions (10^4 to 10^6 s^{-1}). Extracting information on lithium ion conduction from T_1 relaxation data is complicated by various factors which lead to a departure from simple Bloembergen, Purcell and Pound theory. Such factors include anisotropy in the diffusion, structural disorder, and cooperative processes due to the Coulomb interaction, and usually theoretical models for the relaxation must be tailored for the system under study. A large number of examples of ^{6}Li and ^{7}Li relaxation measurements and analyses have been summarized elsewhere, also including applications of spin-echo alignment experiments using Jeener-Broekaert pulse sequences to study slow ionic motions [39]. The latter experiments, which involve monitoring the amplitudes of stimulated echoes over a range of mixing times, can provide access to jump rates in the range $T_1^{-1} < k < T_2^{-1}$, i.e., slow

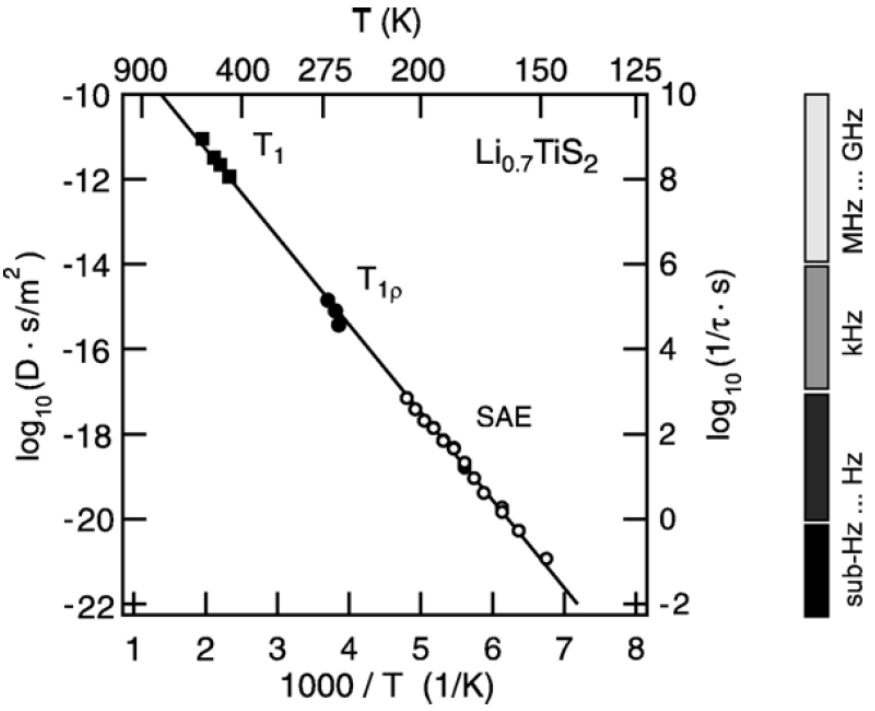

Figure 13 – Lithium ion jump rates (τ^{-1}) determined from a sample of $Li_{0.7}TiS_2$ at various temperatures using different relaxation mechanisms (open circles – spin alignment echoes, closed circles – relaxation under spin-lock fields, closed squares – spin-lattice relaxation). Reproduced with permission from reference 43. Copyright 2006 Elsevier.

and ultra-slow motions on the order of 1 s^{-1}. Figure 13 shows a plot of lithium ion jump rates measured from $Li_{0.7}TiS_2$ using three different relaxation mechanisms [43]. These various relaxation processes allowed the measurement of rates over a range of ten orders of magnitude, a remarkable illustration of the potential sensitivity of NMR relaxation to molecular dynamics.

Lithium ion mobility has also recently been probed in the $Li_3V_2(PO_4)_3$ system using $^6Li\{^{31}P\}$ REDOR (rotational echo double resonance) experiments under magic angle spinning [44]. The pulse sequence involves the observation of a spin-echo from the ^6Li nuclei while rotor-synchronized π-pulses are applied to the ^{31}P nuclei, recoupling the ^6Li-^{31}P dipolar interaction that is otherwise averaged by the sample rotation. Typically, the fraction of signal lost by recoupling is monitored as a function of the dipolar evolution time and the dipolar coupling strength is extracted by fitting the resultant REDOR curve. When dynamics are present, the measured dipolar couplings are reduced in magnitude. In the case of $Li_3V_2(PO_4)_3$, the exchange between the lithium sites was frozen out at low temperatures, leaving a "rattling" mode for the ions within voids in the crystal structure which resulted in a measurable reduction in ^6Li-^{31}P dipolar couplings that could be monitored over a range of temperatures as well as correlated with the local structures via multi-spin simulations [44].

6. Multiple Quantum Experiments.

Multi-dimensional pulse sequences which can achieve high-resolution spectra from quadrupolar nuclei, particularly MQ/STMAS and double quantum experiments, are now being widely applied. As might be expected, phenomena related directly to dynamic processes can be observed in such spectra, and the sensitivity of multiple-quantum experiments to molecular motions is becoming increasingly recognized. In this section we provide several examples for various quadrupolar nuclei.

6.1 Spin I = 1 double-quantum MAS experiments.

Double-quantum (DQ) transitions for I = 1 nuclei ($+1 \leftrightarrow -1$) show increased spectral resolution and no first-order quadrupolar broadening. This has been exploited in

the case of ^2H in a two-dimensional double-quantum MAS experiment to separate the single-quantum (SQ) spinning sideband patterns of chemically resolved deuterons, circumventing the need for selective deuteration. Broadening of the sidebands due to motions of specific deuterons can then be observed for jump rates in the 10^4 to 10^6 s^{-1} range [45]. This technique has been further refined to alias the SQ spinning sidebands into a single centre line by means of rotor synchronization. The resulting correlation of the SQ spectra with the DQ spectra provides a sensitive means of detecting the presence of dynamics on the μs timescale, as illustrated in Figure 14 for oxalic acid dihydrate [46]. The acid group ^2H atoms are effectively static and appear as sharp lines in both SQ and DQ dimensions. The water deuterons, on the other hand, are dynamic and show a drastic broadening in the SQ dimension but a sharp line in the DQ dimension. Since the SQ static quadrupolar linewidth will be on the order of 250 kHz (much larger than a typical MAS rates) reorientational jumps on the μs timescale during the rotor period can change the SQ precession frequency by as much as 10^5 Hz, thereby interfering with the formation of an echo at the end of the rotor period. This reduces the echo intensity and shortens the train of rotary echoes, resulting in broadening. The static DQ linewidth with no quadrupolar broadening is likely to be only a few kHz; therefore any motional jumps will change the frequency by an amount much less than the MAS rate and there is no attenuation of the echo train, hence no broadening.

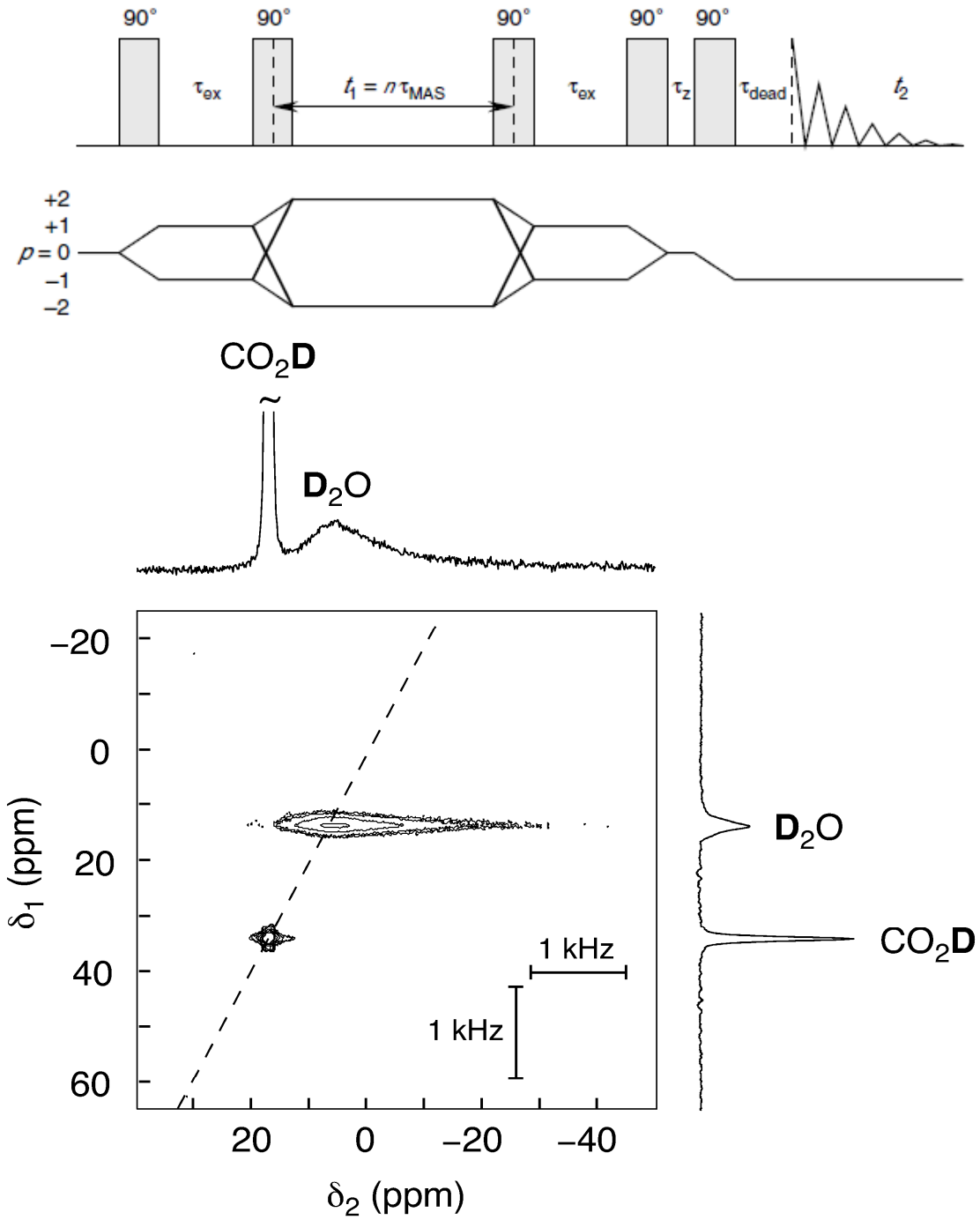

Figure 14. Two-dimensional rotor-synchronized ^{2}H double-quantum MAS NMR. Top: Pulse sequence and coherence pathways. Bottom: Spectrum of oxalic acid dihydrate-d_6 at 9.4 T. In the double-quantum dimension both resonances are sharp,

whereas in the single-quantum dimension the D_2O resonance is broadened by dynamics. Reproduced from reference 46 with permission from Elsevier.

This particular technique can be more sensitive to certain types of motion than the static linewidth experiments described in Section 2.1. For example, the SQ-DQ correlation for hydroxyl-clinohumite ($4Mg_2SiO_4.Mg(OD)_2$) at 314 K shows a SQ linewidth of 524 Hz and a DQ linewidth of only 77 Hz, indicative of dynamics on the μs timescale [47]. However, static ^2H lineshape studies showed little indication of any motion in this system. This can be rationalized in terms of the motional geometry, which involves a re-orientation of the ^2H EFG tensor by 177°. Since this is very close to 180° its effect on the static lineshape was very small, but the motion was clearly detected via the dynamic broadening of the spinning sidebands in the MAS experiment.

A similar phenomenon has been observed when comparing SQ and DQ linewidths for ^{14}N in indirectly-detected ^1H-^{14}N HMQC type experiments [48]. The tripeptide Ala-Ala-Gly contains NH and NH_3^+ groups which show resolved ^{14}N resonances in the DQ $^{14}N/^1H$ correlation spectrum. Significant broadening of the NH_3^+ resonance occurs in the single-quantum dimension, while it remains sharp in the DQ spectrum, once again indicating motion, this time on the 100 ns timescale due to the larger quadrupolar linewidth of ^{14}N.

6.2 MQMAS and STMAS experiments.

The now-common MQMAS technique [49] in the case of spin I = 3/2 nuclei correlates SQ central transitions (+1/2 ↔ −1/2) with triple quantum (TQ) transitions (+3/2 ↔ −3/2). In the two-dimensional spectra obtained the $\delta_1 = 3\delta_2$ diagonal represents the position of the isotropic chemical shift. Resonances with zero quadrupolar coupling will appear on this diagonal, whereas, in the absence of motion or when motions are slower than the Larmor frequency, those with non-zero couplings are shifted off the diagonal by the second-order quadrupolar shift to a lower frequency in δ_2, and by three times this shift to higher frequency in δ_1. As mentioned earlier, if dynamics are occurring with rates comparable to the Larmor frequency, the second-order shift will be affected. At very high dynamic rates this shift will disappear for isotropic motion and will reach a

reduced value corresponding to the effective averaged coupling for anisotropic motion. Consequently, if the off-diagonal peaks are observed to move towards the diagonal as temperature increases, or if the peak is closer to the diagonal than expected based on a known coupling constant, this is clear evidence of very rapid dynamics.

This is illustrated in Figure 15 for ^{11}B MQMAS of the low temperature orthorhombic phase of the pseudo-spherical molecule ortho-carborane ($C_2B_{10}H_{12}$) [26]. The B and C atoms form an icosahedron, but the presence of the two C atoms (in this case adjacent to each other) reduces the true symmetry, and consequently there are four chemically distinct types of B, though the peaks for two of these overlap. The MQMAS spectra show that the off-diagonal resonances move towards the diagonal as the temperature is increased (most evident by comparing the spectra at 223 K and 253 K). In fact, by 253 K the peak for B(9,12) lies directly on the diagonal, indicating an effective averaged coupling constant of zero, while the remaining peaks are still off-diagonal. This implies that the molecule is undergoing very rapid anisotropic motion. The room temperature cubic phase of this material behaves as a plastic crystal, and although MQMAS gave no signals from this phase, a triple-quantum (TQ) ^{11}B-^{1}H MAS correlation experiment demonstrated that all the B atoms undergo very rapid isotropic averaging, since the TQ shifts are all three times larger than the SQ ^{11}B shifts observed in a routine ^{1}H-decoupled MAS spectrum.

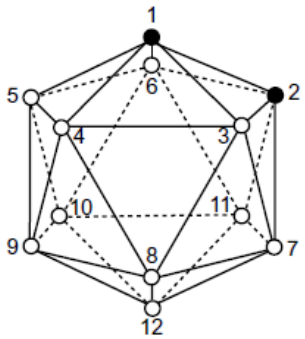

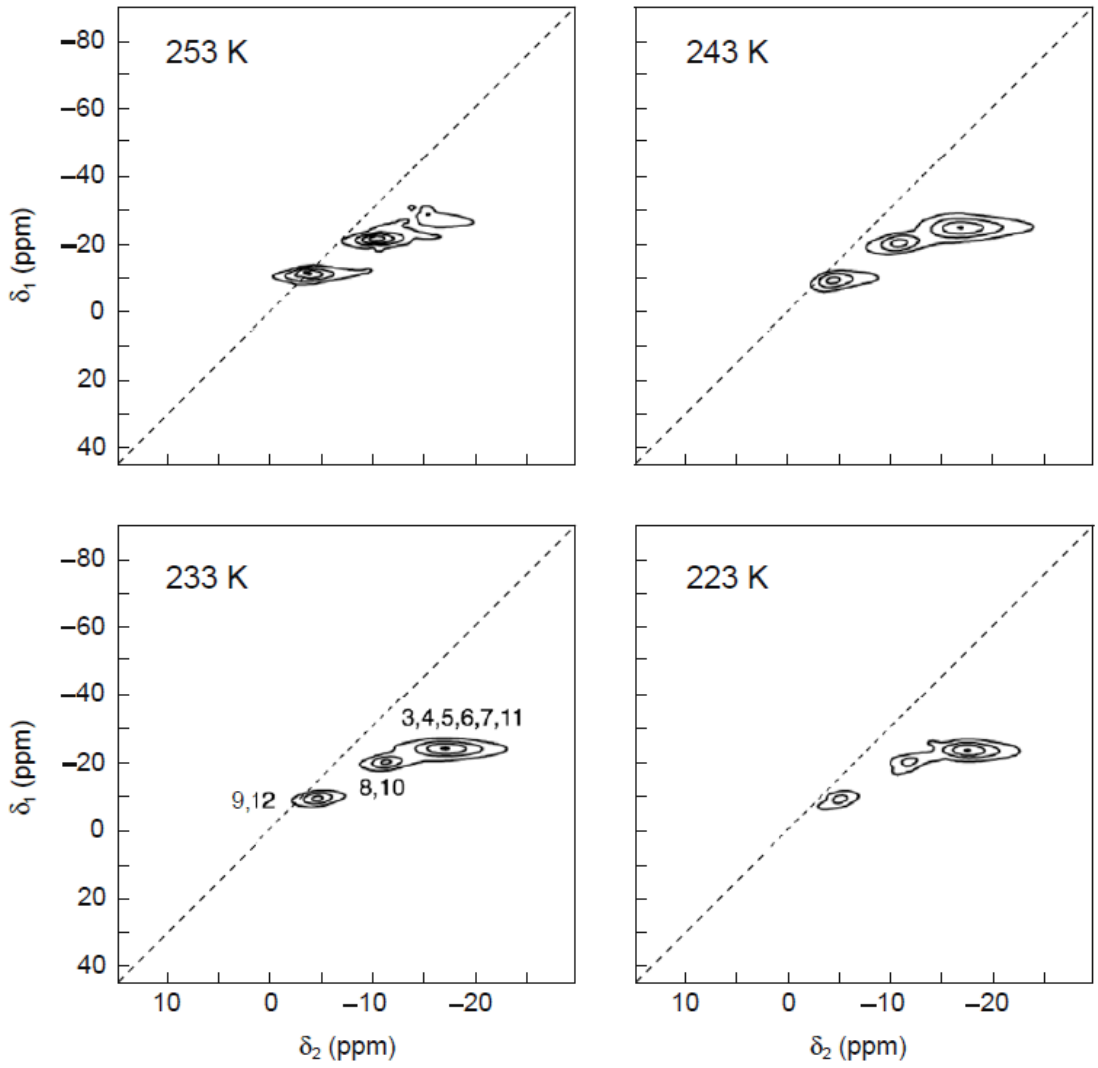

Figure 15. ^{1}H-decoupled ^{11}B MQMAS NMR of ortho-carborane in its low temperature orthorhombic phase as a function of temperature. The dashed line indicates the $\delta_1 = 3\delta_2$ diagonal. Reproduced from reference 26 with permission from Elsevier.

Simulations of MQMAS spectra as a function of jump rate also suggest that in addition to averaging of the second order lineshape in the CT dimension (typically below 10^6 s^{-1}) there will also be a broadening of the TQ linewidths [50]. This is again due to interference of the motion with echo formation but at rates corresponding to the second-

order broadening, but to our knowledge no clear experimental example corresponding to a single activated process is yet available.

For certain jump rates STMAS spectra can be subject to significant dynamic broadening, while the MQMAS spectra for the same material do not appear to suffer any line broadening effects. Examples can be seen in the ^{17}O spectra of hydroxyl-chondrodite and hydroxyl-clinohumite [51,52] where proton hopping motions affect the ^{17}O, and in the ^{27}Al spectra of AlPO-14 materials [53] where calcined-dehydrated AlPO-14 shows sharp spectra but AlPO-14 as-prepared with isopropylamine shows strong broadening in only the STMAS spectra (Figure 16). The explanation for this behavior is similar to that given above for the ^{2}H DQ experiments, where the SQ dimension is subject to the first-order quadrupolar interaction, and fast dynamic jumps interfere with the averaging of this interaction by MAS. In STMAS the satellite transition is subject to the first-order quadrupolar interaction but the STMAS CT transition and both the TQ and CT transitions in MQMAS are not.

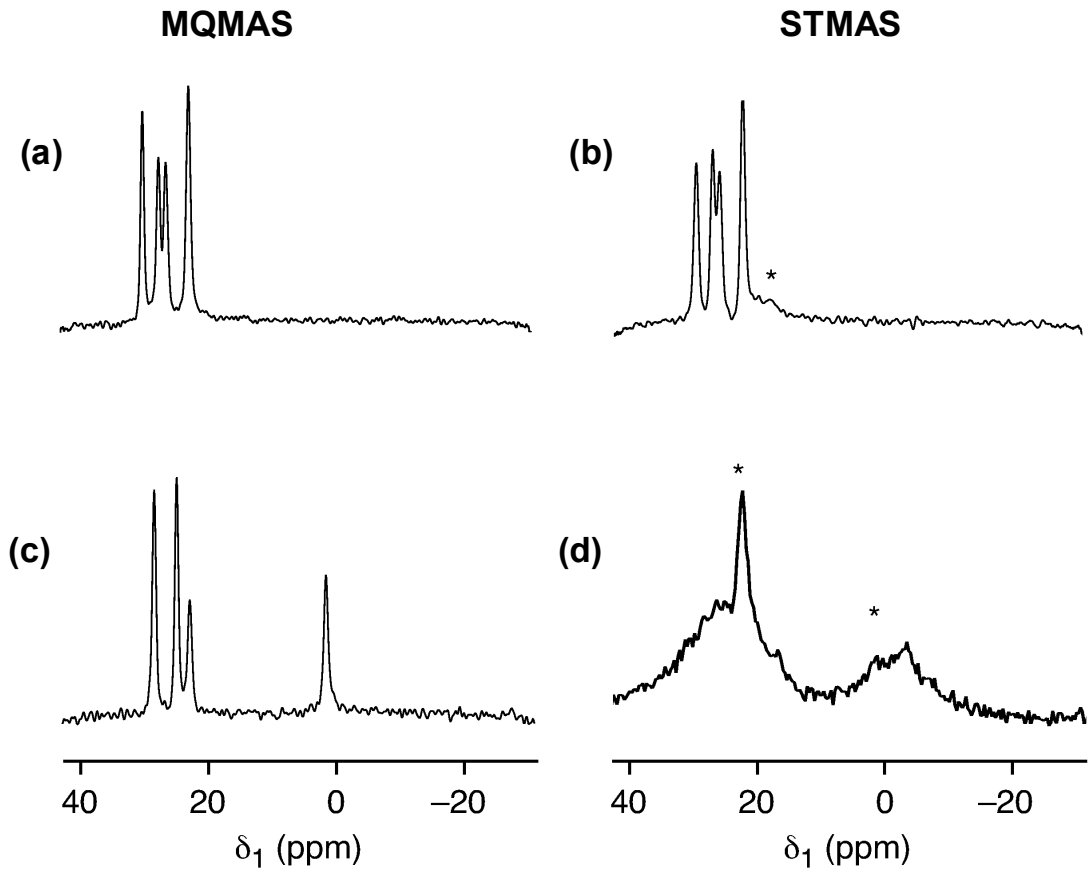

Figure 16. Isotropic projections of ^{27}Al MQMAS (TQ) and STMAS spectra of calcined-dehydrated AlPO-14 (a,b) and AlPO-14-as-prepared with isopropylamine template (c,d), showing dynamic broadening in the STMAS spectrum (d). Reproduced with permission from reference 53. Copyright 2006 American Chemical Society.

7. Concluding Remarks

Quadrupolar NMR plays a vital role in the study of molecular and ionic dynamics in solids, often providing extensive information which cannot be obtained by other techniques, and which is important for understanding the physical properties of materials. It is also important to be aware of the influences that dynamics can have on the quadrupolar NMR spectra of a solid material, since the presence of motion may not necessarily be expected, and could lead to erroneous interpretation of spectra, for example in situations where an apparently isotropic line is not at the isotropic chemical

shift. This article has presented an overview of the current state of this area of research, and with much effort currently focused on the development of solid-state NMR of quadrupolar nuclei there will no doubt be numerous new instances of dynamic effects and new ways of probing them.

References

[1] Abragam A., *The Principles of Nuclear Magnetism*, Clarendon Press, Oxford, 1961, pp 111.

[2] Duer M.J., in *Solid State NMR Spectroscopy Principles and Applications*, Ed. Duer M.J., Blackwell Science, Oxford, 2002, Chp.6.

[3] Tycko R., in *Nuclear Magnetic Resonance Probes of Molecular Dynamics*, Ed. Tycko R., Kluwer Academic, Dordrecht, 1994, Chp.1

[4] Ratcliffe C. I., in "NMR Crystallography", Eds. Harris R. K., Wasylishen R. E. and Duer M. J., John Wiley & Sons Ltd, Chichester, UK, (2009), Chp.24, 355-373 (also appears as emrstm 1040).

[5] Batchelder L.S., Deuterium NMR in Solids, Encyclopedia of Magnetic Resonance, Wiley, vol. 3, (1996) pp. 1574

[6] Meirovitch E. and Freed J.H., Chem. Phys. Lett. 64 (1979) 311-316

[7] Vold R.L. and Hoatson G.L., J. Magn. Reson. 198 (2009) 57-72

[8] Kristensen J.H., Bildsøe H., Jakobsen H.J. and Nielsen N.C., J. Magn. Reson. 100 (1992) 437-443

[9] Maricq M.M. and Waugh J.S., J. Chem. Phys. 70 (1979) 3300-3333

[10] Huang Y., Vold R.L. and Hoatson G.L., J. Chem. Phys. 124 (2006) 104504

[11] Larsen F.H., Jakobsen H.J., Ellis P.D. and Nielsen N.C., Chem. Phys. Lett. 292 (1998) 467-473

[12] Vugmeyster L., Ostrovsky D., Ford J.J. and Lipton A.S., J. Am. Chem. Soc. 132 (2010) 4038-4039

[13] Torchia D.A. and Szabo A., J. Magn. Reson. 49 (1982) 107-121

[14] Hoatson G.L., J. Magn. Reson. 94 (1991) 152-159

[15] Hoatson G.L., Vold R.L. and Tse T.Y., J. Chem. Phys. 100 (1994) 4756-4765

[16] Spiess H.W., J. Chem. Phys. 72 (1980) 6755-6762

[17] Vold R.L., Hoatson G.L., Vugmeyster L., Ostrovsky D. and De Castro P.J., Phys. Chem. Chem. Phys. 11 (2009) 7008-7012
[18] Schmidt C., Wefing S., Blumich B. and Spiess H.W., Chem. Phys. Lett. 130 (1986) 84-90
[19] O'Dell L.A., Prog. Nucl. Magn. Reson. Spec. DOI: 10.1016/j.pnmrs.2011.04.001
[20] Pratum T.K. and Klein M.P., J. Magn. Reson. 81 (1989) 350-370
[21] O'Dell L.A. and Ratcliffe C.I., Chem. Commun. 46 (2010) 6774-6776
[22] Hill E.A. and Yesinowski J.P., J. Chem. Phys. 107 (1997) 346-354
[23] Wasylishen R.E., Pettitt B.A. and Jeffrey K.R., J. Chem. Phys. 74 (1981) 6022-6026
[24] Kristensen J.H. and Farnan I., J. Chem. Phys. 114 (2001) 9608-9624
[25] Schurko R.W., Wi S. and Frydman L., J. Phys. Chem. A 106 (2002) 51-62
[26] Kurkiewicz T., Thrippleton M.J. and Wimperis S., Chem. Phys. Lett. 467 (2009) 412-416
[27] Kristensen J.H. and Farnan I., J. Magn. Reson. 158 (2002) 99-125
[28] Larsen F.H., J. Magn. Reson. 171 (2004) 293-304
[29] Witschas M., Eckert H., Freiheit H., Putnis A., Korus G. and Jansen M., J. Phys. Chem. A 105 (2001) 6808-6816
[30] Ba Y., Ripmeester J.A. and Ratcliffe C.I., Can. J. Chem. (2011) in press
[31] Wittebort R.J., Usha M.G., Ruben D.J., Wemmer D.E. and Pines A., J. Am. Chem. Soc. 110 (1988) 5668-5671
[32] Moudrakovski I.L., Ratcliffe C.I. and Ripmeester J.A., J. Am. Chem. Soc., 123 (2001) 2066-2067.
[33] Witschas M.and Eckert H., J. Phys. Chem. A 103 (1999) 10764-10775
[34] Kim N. and Grey C.P., Science 297 (2002) 1317-1320
[35] Hampson M.R., Hodgkinson P., Evans J.S.O., Harris R.K., King I.J., Allen S. and Fayon F., Chem. Commun. (2004) 392-393
[36] Hodgkinson P. and Hampson M.R., Solid State Nucl. Magn. Reson. 30 (2006) 98-105
[37] Andrew E.R. and Tunstall D.P., Proc. Phys. Soc. 78 (1961) 1-11
[38] Gordon M.I. and Hoch M.J.R., J. Phys. C: Solid State Phys. 11 (1978) 783-795

[39] Böhmer R., Jeffrey K.R. and Vogel M., Prog. Nucl. Magn. Reson. Spec. 50 (2007) 87-174

[40] Brinkmann D., Mali M., Roos J., Messer R. and Birli H., Phys. Rev. B 26 (1982) 4810-4825

[41] Xu Z. and Stebbins J.F., Science 270 (1995) 1332-1334

[42] Bloembergen N., Purcell E.M. and Pound R.V., Phys. Rev. 73 (1948) 679-712

[43] Wilkening M. and Heitjans P., Solid State Ionics 177 (2006) 3031-3036

[44] Cahill L.S., Kirby C.W. and Goward G.R., J. Phys. Chem. C 112 (2008) 2215-2221

[45] Duer M.J. and Stourton C., J. Magn. Reson. 129 (1997) 44-52

[46] Cutajar M., Ashbrook S.E. and Wimperis S., Chem. Phys. Lett. 423 (2006) 276-281

[47] Griffin J.M., Miller A.J., Berry A.J., Wimperis S. and Ashbrook S.E., Phys. Chem. Chem. Phys. 12 (2010) 2989-2998

[48] Cavadini S., Abraham A., Ulzega S. and Bodenhausen G., J.Am. Chem. Soc. 130 (2008) 10850-10851

[49] Frydman L., Harwood J.S., J.Am. Chem. Soc. 117 (1995) 5367-5368

[50] Kotecha M., Chaudhuri S., Grey C.P. and Frydman L., J. Am. Chem. Soc., 127 (2005) 16701-16712.

[51]Ashbrook S.E., Antonijevic S., Berry A.J. and Wimperis S., Chem. Phys. Lett., 364 (2002) 634-642.

[52] Griffin J.M., Wimperis S., Berry A.J., Pickard C.J. and Ashbrook S.E., J. Phys. Chem., 113 (2009) 465-471.

[53] Antonijevic S., Ashbrook S.E., Biedasek S., Walton R.I., Wimperis S. and Yang H., J. Am. Chem. Soc., 128 (2006) 8054-8062.

Brief biographies:

Luke A. O'Dell received his PhD from the University of Warwick, UK, in 2007. He subsequently carried out post-doctoral research in solid-state NMR with Prof. Mark Smith (Warwick) and Prof. Robert Schurko (University of Winsdor, Ontario, Canada), before joining the Steacie Institute for Molecular Sciences (NRC Canada) in 2009 as a

Research Associate. His current interests lie primarily in the development of solid-state NMR techniques for insensitive quadrupolar nuclei, particularly ^{14}N.

Christopher Ian Ratcliffe. *b* 1951. B.Sc.(Hons.), 1972, Ph.D., 1975, University of Durham, UK. Trained in solid state NMR during post-doctoral work (University of British Columbia), and as a Research Associate at the National Research Council of Canada. He joined NRC in 1982 where he is currently a Senior Research Officer and leader of the Materials Structure and Function Program. Approx. 257 publications. Current research focus: hydrogen storage materials, nanoporous materials, nanoconfinement, applications of ^{129}Xe NMR, order/disorder and dynamics in solids, host-guest materials, clathrate hydrates.

Contact Information :

Luke O'Dell
Phone: 1-613-990-1566
Email: luke.odell@nrc-cnrc.gc.ca

Chris Ratcliffe
Phone : 1-613-991-1240; FAX : 1-613-998-7833
Email: chris.ratcliffe@nrc-cnrc.gc.ca

Keywords: dynamics, quadrupolar nuclei, electric field gradients, reorientation, translation, MQMAS, STMAS